Planta (2001) 214: 142–152
DOI 10.1007/s004250100601

ORIGINAL ARTICLE

R.B. Peterson · E.A. Havir

Photosynthetic properties of an *Arabidopsis thaliana* mutant possessing a defective PsbS gene

Received: 2 March 2001 / Accepted: 16 March 2001 / Published online: 28 June 2001

Abstract We describe the properties of *npq4-9*, a new mutant of *Arabidopsis thaliana* (L.) Heynh. with reduced nonphotochemical quenching (NPQ) capacity that possesses a single amino acid substitution in the PsbS gene encoding PSII-S, a ubiquitous pigment-binding protein associated with photosystem II (PSII) of higher plants. Growth, photosynthetic pigment contents, and levels of the major PSII antenna proteins were not affected by *npq4-9*. Although the extent of de-epoxidation of violaxanthin to antheraxanthin plus zeaxanthin for leaves displaying the mutant phenotype equaled or exceeded that observed for the wild type, the relative effectiveness of de-epoxidized xanthophylls in promoting NPQ was consistently lower for the mutant. Energy partitioning in PSII was analyzed in terms of the competition for singlet chlorophyll *a* among the processes of fluorescence, thermal dissipation, and photochemistry. The key processes of NPQ and photochemistry in open PSII centers are represented by the relative in vivo rate constants k_N and k_{P0}, respectively. The magnitude of k_{P0} in normal leaves declined only slightly with increasing k_N, consistent with localization of NPQ primarily in the antenna complex. Conversely, a highly significant linear decline in k_{P0} with increasing k_N was observed for the mutant, consistent with a role for the PSII reaction center in the NPQ mechanism. Although the PSII absorption cross-section for white light was not significantly different relative to that of the wild type, PSII quantum yield was significantly lower in the mutant. The resulting lower capacity for linear electron transport in the mutant primarily affected reduction of terminal acceptors other than CO_2. Parallel measurements of fluorescence and in vivo absorbance at 820 nm indicated a consistently higher steady-state level of reduction of PSII acceptors and accumulation of $P700^+$ for the mutant. This suggests that inter-photosystem electron transport in the mutant is restricted either by a higher transthylakoid ΔpH or by diminished accessibility to reduced plastoquinone.

Keywords *Arabidopsis* (mutant, photosynthesis) · Chlorophyll fluorescence · Energy dissipation · Photosynthesis · Photosystems I, II · Zeaxanthin

Abbreviations A: net CO_2 assimilation rate (μmol m^{-2} s^{-1}); · α: absorption coefficient; · ANOVA: analysis of variance; · Anth: antheraxanthin; · a_2: absorption cross-section for PSII; · A820: in vivo absorbance at 820 nm; · Chl: chlorophyll; · F_{0d} and F_0': minimum fluorescence yield (all PSII traps open) in the dark-adapted and light-adapted states, respectively; · F_{md} and F_m': maximum fluorescence yield (all PSII traps closed) in fully dark-adapted and light-adapted states, respectively; · F_v: (F_{md}–F_{0d}); · F_s: steady-state fluorescence yield; · I_a: photon absorption rate (μmol m^{-2} s^{-1}); · J_c: electron transport rate (μmol $m^{-2}s^{-1}$) in support of CO_2 fixation plus photorespiration; · J_t: total electron transport rate; · k_f, k_{P0}, k_d, k_N: relative rate constants for de-excitation of singlet Chl in PSII by fluorescence, photochemistry in open centers, non-regulated thermal dissipation, and H^+-dependent thermal conversion, respectively; · q_P: fraction of PSII centers in the open state [(F_m'–F_s)/(F_m'–F_0')]; · Viol: violaxanthin; · WT: wild type Landsberg *erecta*; · Zea: zeaxanthin; · $\phi(O_2)$: photochemical yield of O_2 evolution [mol O_2 (mol quanta)$^{-1}$]; · ϕ_2: photochemical yield of PSII [(F_m'–F_s)/F_m']

Introduction

PSII possesses the unique ability to alter rapidly and reversibly the capacity to capture quanta necessary for the photolysis of H_2O, which constitutes the first in a series of reactions culminating in reduction of CO_2 to

R.B. Peterson (✉) · E.A. Havir
Department of Biochemistry and Genetics,
The Connecticut Agricultural Experiment Station,
123 Huntington St., New Haven, CT 06511, USA
E-mail: richard.peterson@po.state.ct.us
Fax: +1-203-9748502

carbohydrate. A potential excess of 50% of the radiant energy absorbed by PSII is converted to heat in a process commonly referred to as nonphotochemical quenching (NPQ). Localization of NPQ in the antenna system constitutes an efficient means of protecting reaction centers from overstimulation that could result in formation of reactive singlet O_2 (Melis 1999). Hence, NPQ should mitigate photoinactivation associated with over-reduction of PSII acceptor pools (Hurry et al. 1996).

The mechanism of NPQ involves H^+ and carotenoids. The energy-storing transthylakoid pH gradient links energy consumption by the dark reactions of photosynthesis and energy dissipation in the PSII light-harvesting complex. The dominant, rapidly relaxing component of NPQ (i.e. q_E) is most clearly associated with the pH gradient (Horton et al. 1996). Accumulation of the xanthophylls antheraxanthin (Anth) and zeaxanthin (Zea) correlates with increases in NPQ (Demmig et al. 1987). Direct evidence for involvement of xanthophylls, including lutein, in the NPQ mechanism is provided by mutants of *Chlamydomonas* and *Arabidopsis* deficient in xanthophyll-cycle activities (Niyogi et al. 1997, 1998; Pogson et al. 1998).

An important recent finding is that mutational loss of the PSII-S protein (CP22) encoded by the PsbS gene results in substantial loss of NPQ capacity in *Arabidopsis* (Li et al. 2000). The PSII-S protein possesses homology with other chlorophyll (Chl) *a*/*b* proteins and reportedly binds four to six Chl molecules and one carotenoid (Funk et al. 1995; Jansson 1999). Interestingly, violaxanthin (Viol) has been detected in purified PSII-S but in sub-stoichiometric amounts (Funk et al. 1995). The PSII-S deletion mutant *npq4-1* showed an 80% reduction in NPQ capacity but retained normal PSII quantum yield, xanthophyll cycle activity, and tolerance to high light (Li et al. 2000). The original description of *npq4-1* was followed by a description of another PSII-S mutant allele, now renamed *npq4-8*, which displayed similar properties (Peterson and Havir 2000). The apparent absence of effects on growth and leaf pigment composition in these mutants indicates a specific role for PSII-S in the NPQ mechanism, yet no obligatory function with regard to light harvesting or electron transport.

In this report we describe properties of a new NPQ-deficient mutant of *Arabidopsis*, *npq4-9*, which possesses a single amino acid substitution in the PsbS gene. We evaluate energy utilization in PSII in terms of a monopartite model in which various deactivation processes compete for singlet Chl (Dau 1994). Accordingly, this competition can be described in terms of relative rate constants for fluorescence (k_f), basal unregulated thermal deactivation (k_d), photochemistry in open centers (k_{P0}), and nonphotochemical quenching (k_N) where $k_f + k_d = 1$ (Laisk et al. 1997; Laisk and Oja 1998). This unempirical approach provides valuable insights into the contrasts between the wild type (WT) and mutant with regard to PSII function in vivo. Finally, we show that the *npq4-9* mutation causes a profound decrease in the photochemical quantum yield of PSI. Effects of *npq4-9* on the redox state of PSI appear to involve a change in the way inter-photosystem electron transport is regulated. These changes, in turn, mediate alterations in the allocation of electrons to CO_2 versus alternate acceptors compared to normal leaves.

Materials and methods

Plant material and growth conditions

Seeds of *Arabidopsis thaliana* (L.) Heynh. (ecotype Landsberg *erecta*), mutagenized by treatment with ethylmethanesulfonate, were obtained from Lehle Seeds (Round Rock, Tex., USA). Four- to six-day-old seedling populations were screened for putative NPQ-deficient variants by fluorescence imaging (Peterson and Havir 2000). One line (*npq4-9*) was backcrossed to the WT three times. Homozygosity for the mutant allele *npq4-9* was confirmed by fluorescence imaging. Plants were grown in a commercial potting mixture in a growth chamber fitted with Cool White and incandescent lamps at an irradiance of 125 μmol quanta $m^{-2}s^{-1}$. The day:night cycle was 16 h:8 h with corresponding temperatures of 23 °C:20 °C. Fully expanded leaves (1.5–2.5 cm^2 in area) were selected from WT and mutant plants at the rosette stage of development.

Gas-exchange measurements

The Fast Response Gas Exchange Measurement System was employed to simultaneously measure gas exchange and optical signals in leaves under highly controlled environmental conditions (Laisk and Oja 1998). The apparatus supports two independent gas streams. A system of pressure regulators, precision orifices, and manostats blend pure N_2, O_2, and CO_2 in each stream. Humidity is controlled by diversion of a selectable portion of the flow through a humidifier followed by re-joining of the gas streams. The water vapor pressure deficit was maintained at approximately 15 mbar. Electronically controlled valves direct a selected gas stream (channel) either through the leaf chamber or to a bypass. Hence, instrumental baselines for the measuring channel (channel 2) were conveniently recorded while the chamber was flushed by channel 1 (maintained at 360 μmol mol^{-1} CO_2, 21% O_2, balance N_2 in these experiments). The gas flow rate in each channel was fixed at 0.5 mmol s^{-1}. A Licor LI-6252 CO_2 analyzer and an Ametek S-3A/II O_2 analyzer each equipped with flow-through cells were installed downstream from the leaf chamber in channel 2. Both analyzers operated in absolute mode. Transpiration was measured by means of an inline micropsychrometer. Leaf substomatal CO_2 concentration (C_i) is expressed as the dissolved aqueous phase molarity of CO_2 in equilibrium with the internal gas-phase CO_2 partial pressure calculated from CO_2 and H_2O exchange. Analog signals from CO_2 and O_2 analyzers, micropsychrometer, and optical system were converted to digital data at 5-ms intervals and averaged over 200 ms using an ADIO1600 A/D board (ICS Advent, San Diego, Calif., USA) installed in an IBM-compatible pentium computer. See Laisk and Oja (1998) for further details.

The leaf-chamber design ensures a rapid system response to changes in leaf gas exchange, uniform illumination, and a stable leaf temperature. Distilled H_2O was provided to the cut end of an excised *Arabidopsis* leaf through a stainless-steel tube (1-mm i.d.) extending from the exterior to the interior of the chamber. The upper surface of the leaf was affixed to the transparent glass wall of the chamber with agar paste. Gas exchange occurred solely via the underside of the leaf. The glass wall is common with a jacket containing flowing water maintained at 23.0 °C. Heat-budget calculations showed that leaf temperature varied by no more than 0.1 °C relative to that of the water jacket.

Optical measurements

The optical system is composed of an array of 1-mm-diameter plastic fibers terminating in a common plane 15 mm from the upper surface of the leaf. Separate fiber bundles extend to the: (i) actinic light source, (ii) fluorescence measuring beam emitter, (iii) fluorescence detector, (iv) saturating flash (15,000 μmol quanta $m^{-2}s^{-1}$) source for measurement of maximum fluorescence yield (F_m), (v) A820 measuring-beam source, and (vi) source of saturating far-red illumination (filter 720FS10.25; Andover Corp, Salem, N.H., USA). A seventh fiber bundle joined the A820 detector to the opposite side of the chamber for assessment of transmission of the A820 measuring beam by the leaf. Separate Schott electronic KL1500 sources provided light for the actinic, saturating flash, and far-red beams. White light sources were fitted with heat-reflecting filters (OCLI, Santa Rosa, Calif., USA). The incident actinic irradiance (I_o) was controlled by varying the power to the tungsten-halogen lamp. An eighth fiber bundle connected to a Licor LI-190SB quantum sensor provided a continuous recording of I_o (400–700 nm).

Pulse-modulated Chl fluorescence-yield measurements were conducted with the PAM 101 system (H. Walz, Effeltrich, Germany). The system employed an ED-101BL emitter-detector unit, which utilizes a blue-light-emitting diode to excite fluorescence. A filter slide attached to the unit permits selective detection of either the far-red (>710 nm) or red (660–710 nm) region of the room-temperature fluorescence emission spectrum. Unless stated otherwise, all measurements were obtained in the far-red range. Minimal fluorescence yields, F_{0d} and F_0', in the dark-adapted and light-adapted states, respectively, were recorded at a measuring beam modulation frequency of 1.6 kHz. All other fluorescence-yield levels were measured at a modulation frequency of 100 kHz. Measurement of F_0' in darkness was preceded by 3 s of illumination with far-red light to oxidize the PSII acceptor side. The steady-state maximal fluorescence yield F_m' was assessed as the peak signal recorded during a 1.5-s saturating pulse of white light. Fluorescence signals were corrected for effects of residual detector sensitivity to the measuring beam, slight overload of the detector during saturating pulses, and incomplete reduction of the PSII electron acceptor side during measurement of F_m'. In addition, the level of the invariant fluorescence yield arising from PSI was subtracted from all fluorescence-yield measurements prior to calculation of PSII light-utilization parameters (Genty et al. 1990). Further details pertaining to measurement and application of these corrections will be presented elsewhere.

Measurement of the redox state of P700 was based on the in vivo light-dark absorbance change at 820 nm. A Walz ED800T emitter-detector unit was used in conjunction with a separate PAM 101 main control unit (Schreiber et al. 1988). The [$P700^+$] is proportional to the rapid initial ΔA820 observed following interruption of the actinic beam. Saturating far-red illumination was added to assess the signal associated with full photooxidation of P700 to $P700^+$ (i.e., $\Delta A820_{max}$). A typical A820 recording and the method for calculation of $\Delta A820/\Delta A820_{max}$ are shown in Fig. 1.

The rate of photon absorption (I_a) by a leaf is related to I_o by the absorption coefficient α (i.e., $I_a = \alpha I_o$). To measure α, a leaf was mounted on a sliding mechanism inside a 10-cm-diameter integrating sphere (Labsphere, North Sutton, N.H., USA). An LI-190SB quantum sensor was mounted in a wall port of the sphere. A narrow beam of white light (≤100 μmol quanta $m^{-2}s^{-1}$) was admitted via a pinhole. The quantum sensor reading was recorded with either the leaf sample (Q_l) or a filter-paper replica (Q_r) in the path of the beam. Hence, $\alpha = (1 - Q_l/Q_r)$.

Experimental protocols

Measurements of F_{0d} and F_{md} were preceded by at least 1 h of dark-adaptation. Effects of CO_2 concentration on leaf steady-state photosynthetic properties were recorded following 1 h of pre-illumination in channel 1 at an incident irradiance of 110 μmol quanta $m^{-2}s^{-1}$. Measurements in channel 2 were recorded sequentially at external gas phase CO_2 levels of 80, 60, 40, 20, 10, 100, 200, 300, 400, 500, 600, 700, 800, 900, 1,000, and 300 μmol mol^{-1} in 1.0% O_2 at the same irradiance. These measurements were then repeated for $I_o = 510$ μmol quanta $m^{-2}s^{-1}$. Separate measurements of the dependence of O_2 evolution on irradiance were conducted at I_o levels ranging from 20 to 80 μmol quanta m^{-2} s^{-1} in 500 μmol CO_2 mol^{-1} (background [O_2] of ≈15 μmol mol^{-1}). The total rate of PSII electron transport (J_t) was calculated as:

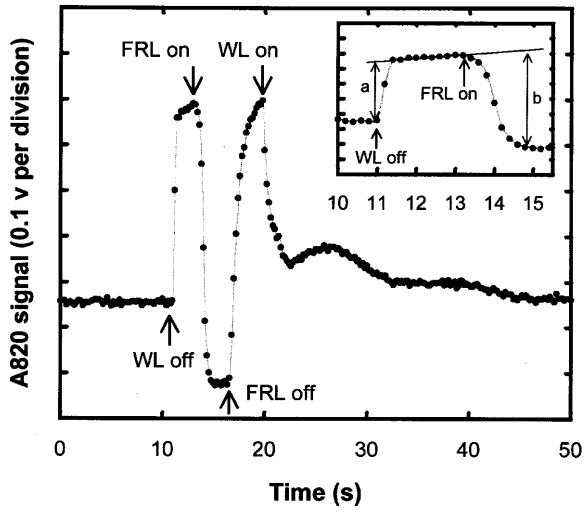

Fig. 1 Typical recording (200-ms intervals) of changes in A820 observed during determination of the steady-state in vivo level of oxidation of P700 for a WT *Arabidopsis thaliana* leaf. Actinic white light (510 μmol quanta $m^{-2}s^{-1}$) was interrupted (*WL off*) and saturating far-red light was added 2 s later (*FRL on*). After attainment of a steady-state A820, the far red light was switched off (*FRL off*) and actinic illumination was restored (*WL on*) after 3 s of darkness. The signal changes corresponding to (*a*) and (*b*) in the *inset* illustrate how ΔA820 values corresponding to the steady-state [$P700^+$] (i.e., ΔA820) and total [P700] (i.e., $\Delta A820_{max}$) are assessed, respectively

$$J_t = \alpha a_2 \phi_2 I_o \quad (1)$$

where a_2 is the PSII absorption cross-section and ϕ_2 is the photochemical yield of PSII [$(F_m'-F_s)/F_m'$; Genty et al. 1989]. Electron transport rates associated with net fixation of CO_2 plus photorespiration (J_c) were calculated according to Laisk and Oja (1998), i.e.

$$J_c = 4(A + R_d)\frac{2K_sC_i + 2O_i}{2K_sC_i - O_i} \quad (2)$$

where A is the rate of net CO_2 assimilation expressed on the basis of leaf area, R_d is mitochondrial "dark" respiration in the light, K_s is the CO_2/O_2 specificity factor of ribulose-1,5-bisphosphate carboxylase-oxygenase (Rubisco), and O_i is the concentration of dissolved O_2 (14 μM). Since individual *Arabidopsis* leaves did not fill the illuminated area (10 cm^2) within the chamber it was necessary to measure leaf area directly. Excised leaves were elliptical in shape, so area was calculated from measurements of leaf dimensions (i.e., $\pi/4 \times$ length $\times$ width).

Relative rate constants for photochemistry in open PSII centers, k_{P0}, and for ΔpH-dependent thermal de-excitation, k_N, were calculated as:

$$k_{P0} = \frac{F_{md}}{F_0'} - \frac{F_{md}}{F_m'} \quad (3)$$

and

$$k_N = \frac{F_{md}}{F_m'} - 1 \quad (4)$$

In the derivation of these equations it is assumed that the sum of the rate constants for fluorescence emission, k_f, and biologically unregulated thermal conversion, k_d, is unity (Laisk et al. 1997; Laisk and Oja 1998). Note that for the dark-adapted state F_{0d} and F_{md} are substituted for F_0' and F_m', respectively, in Eq. 3.

Pigment analysis and molecular procedures

Extraction of leaf samples and quantitation of photosynthetic pigments was conducted as described previously (Peterson and Havir 2000). For immunoblots, leaf samples were ground in liquid N_2 and extracted with 10 mM Tris, 2 mM EDTA, pH 7.5. The resulting pellet fraction was extracted with acetone. Prior to SDS-PAGE the pellet was treated by boiling in 32 mM Tris-HCl, 1% SDS, 2.5% 2-mercaptoethanol, 5% glycerol, pH 6.8. Electrophoresis and antibody treatments were performed as described previously (Peterson and Havir 2000). Quantitative analysis of immunoblots was based on scans of digital images using ImageJ (http://rsb.info.nih.gov/ij). DNA sequencing of the PsbS gene from WT and *npq4-9* plants was performed in the laboratory of Dr. K.K. Niyogi (University of California, Berkeley, USA) using standard procedures including amplification by the polymerase chain reaction.

Results

The *npq4-9* mutation in relation to PsbS gene expression and structure

Genotypes *NPQ4-9:NPQ4–9*, *NPQ4-9:npq4-9*, and *npq4-9:npq4-9* were observed in the proportion of 18:35:20, respectively, in an F_2 population derived from a cross of a non-segregating mutant parent with WT. We conclude that the mutation segregates as a simple nuclear trait and note that its expression is semidominant. The *npq4-9* mutation mapped to the PsbS locus as did the NPQ-deficient mutation *npq4-8* described previously (Peterson and Havir 2000). Figure 2A shows a Western blot of solubilized thylakoid membranes from plants homozygous for the *npq4-9* mutation in relation to the WT. The *npq4-9* mutation is associated with two distinct bands, one essentially identical in apparent molecular weight to the single band found for the WT and a second band approximately 500 Da larger. Quantitative scanning densitometry (Fig. 2A) revealed that the total extent of cross-reaction with anti-PsbS was identical for WT and mutant (based on the means of three replicate preparations for each, SE = 8%). Likewise, 61.4 ± 4.3% and 38.6 ± 4.6% of the signal was associated with the faster and slower bands, respectively, of the mutant. Hence, the ratio of the faster:slower bands is 1.6. Figure 2B shows the DNA sequence of the translated portion of the PsbS gene from the WT and the *npq4-9* mutant in relation to the GenBank cDNA clone AF134131 (ecotype Columbia). Four silent base changes were observed plus a G-to-A change at position 339 for *npq4-9*. The latter results in substitution of an aspartate residue for glycine at position 100 in the first membrane-spanning domain of the native PSII-S protein (Jansson 1999). Analysis of the PSII-S cDNA sequence using NetPhos 2.0 (http://www.cbs.dtu.dk) indicated the presence of

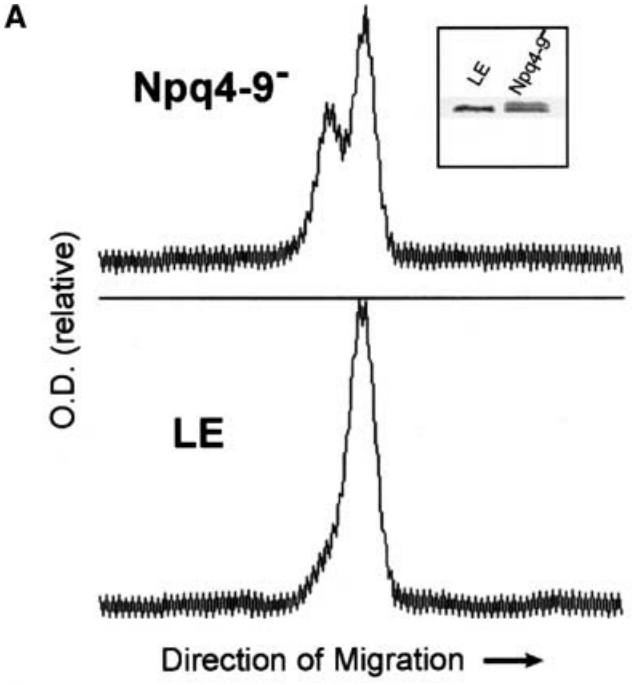

B

41	ATG	GCT	CAA	ACC	ATG	CTG	CTT	ACT	TCA	GGC	GTC
74	ACC	GCC	GGC	CAT	TTT	TTG	AGG	AAC	AAG	AGC	CCT
107	TTG	GCT	CAG	CCC	AAA	GTT	CAC	CAT	CTC	TTC	CTC
							(160, T)				
140	TCT	GGA	AAC	TCT	CCG	GTT	GCA	CTA	CCA	TCT	AGG
173	AGA	CAA	TCA	TTC	GTT	CCT	CTC	GCT	CTC	TTC	AAA
206	CCC	AAA	ACC	AAA	GCT	GCT	CCT	AAA	AAG	GTT	GAG
239	AAG	CCG	AAG	AGC	AAG	GTT	GAG	GAT	GGC	ATC	TTT
						(289, A)					
272	GGA	ACG	TCT	GGT	GGG	ATT	GGT	TTC	ACA	AAG	GCG
305	AAT	GAG	CTA	TTC	GTT	GGT	CGT	GTT	GCT	ATG	ATC
	(339, A*)										
338	GGT	TTC	GCT	GCA	TCG	TTG	CTT	GGT	GAG	GCG	TTG
									(397, A)		
371	ACG	GGA	AAA	GGG	ATA	TTA	GCT	CAG	CTC	AAT	CTG
404	GAG	ACA	GGG	ATA	CCG	ATT	TAC	GAA	GCA	GAG	CCA
437	TTG	CTT	CTC	TTC	TTC	ATC	TTG	TTC	ACT	CTG	TTG
470	GGA	GCC	ATT	GGA	GCG	CTC	GGA	GAC	AGA	GGA	AAA
503	TTC	GTC	GAC	GAT	CCT	CCC	ACC	GGG	CTC	GAG	AAA
536	GCC	GTC	ATT	CCT	CCC	GGC	AAA	AAC	GTC	CGA	TCT
	(571, T)										
569	GCC	CTC	GGT	CTC	AAA	GAA	CAA	GGT	CCA	TTG	TTT
602	GGG	TTC	ACG	AAG	GCG	AAC	GAG	TTA	TTC	GTA	GGA
635	AGA	TTG	GCA	CAG	TTG	GGA	ATA	GCA	TTT	TCA	CTG
668	ATA	GGA	GAG	ATT	ATT	ACC	GGG	AAA	GGA	GCA	TTA
701	GCT	CAA	CTC	AAC	ATT	GAG	ACC	GGT	ATA	CCA	ATT
734	CAA	GAT	ATC	GAA	CCA	CTT	GTC	CTC	TTA	AAC	GTT
767	GCT	TTC	TTC	TTC	TTC	GCT	GCC	ATT	AAT	CCT	GGT
800	AAT	GGA	AAA	TTC	ATC	ACC	GAT	GAT	GGT	GAA	GAA
833	AGC	TAA									

Fig. 2 **A** Typical densitometric scans of immunoblots (*inset*) against the PsbS gene product for solubilized thylakoid membranes obtained from the *npq4-9* mutant and WT (*LE*) of *Arabidopsis*. The leaf extract samples employed in this figure corresponded to 2.2 μg total Chl each for WT and mutant. Replicate sample sizes were adjusted so as to be within the linear range of response of the detection system. **B** The DNA sequence of the coding region of the PsbS gene [nucleotides 41–838 of GenBank accession AF134131 (ecotype Columbia)]. Base changes for the WT and *npq4-9* are *highlighted*. Changes at positions 160, 289, 397, and 571 are silent and found in both the WT and the mutant. The G-to-A change at position 339 (denoted by *) is assumed to correspond to the *npq4-9* mutation

three phosphorylation sites in the mature polypeptide but no glycosylation sites. Comparison of the cDNA sequence with the corresponding genomic sequence (BAC T18F15) revealed the presence of three introns that were 84, 79, and 466 nucleotides in length.

Effects of *npq4-9* on PSII function and leaf photosynthesis

Table 1 summarizes a number of properties relevant to photosynthetic performance in the WT and the mutant phenotype (Npq4-9$^-$). Pigment distribution and respiratory activities were unaffected by the mutation. As reported previously for *npq4-8* (Peterson and Havir 2000), no differences between WT and *npq4-9* were observed in the levels of the PSII light-harvesting proteins Lhcb1–6 (not shown). No difference was detected in the fixed level of fluorescence at wavelengths >710 nm that arises from PSI (Genty et al. 1990; Pfündel 1998). Although both the total Chl content per unit leaf area and the leaf absorption coefficient (α) were on average slightly lower in the mutant relative to the WT these differences were not statistically significant ($P > 0.05$). Stomatal resistance to CO_2 diffusion was modestly higher in the mutant at high irradiance only. Significant differences were found for indicators of PSII function. The PSII photochemical yield for dark-adapted leaf material (F_v/F_{md}) was 4% lower while the quantum yield for O_2 evolution in limiting light, $\phi(O_2)$, was reduced by 22%. Figure 3 shows that PSII quantum yield based on fluorescence (ϕ_2) declined in both WT and mutant plants as CO_2 levels became limiting and more energy was allocated to thermal dissipation and fluorescence. Values of ϕ_2 for the mutant were consistently lower at both irradiance levels and over the entire range of C_i values tested (0.25 μM to approximately 30 μM). Two way analysis of variance (ANOVA) indicated that average ϕ_2 values for the mutant were 8% and 16% lower for the mutant compared to the WT at low (slightly less than that used for growth) and high (4 times that used for growth) irradiance, respectively. Measurements of the steady-state ΔA820 (Fig. 3) revealed that levels of $P700^+$ were consistently higher for Npq4-9$^-$ indicating a lower quantum yield for PSI (Weis and Lechtenberg 1989).

The *npq4-9* mutation was originally detected while screening *Arabidopsis* seedlings for variants defective in the apparent ability to promptly induce NPQ when challenged with excess illumination (Peterson and Havir 2000). Figure 4 compares the rate constant for regulated thermal conversion (k_N, Eq. 4) and extent of xanthophyll de-epoxidation for the WT and Npq4-9$^-$. Surprisingly, at the two lowest irradiance levels of Fig. 4, k_N was approximately 50% higher for the mutant than for WT. However, the extent of xanthophyll de-epoxidation for the mutant was on average 2-fold that of the WT under these conditions. Only at the highest irradiance level employed was k_N significantly lower in Npq4-9$^-$ than in the WT. The results clearly show that, despite the interactive effects of irradiance and genotype described, a given [Anth + Zea] is less effective in promoting nonphotochemical quenching in the mutant.

Figure 5 compares k_N levels as a function of C_i at low and high irradiance. When irradiance was excessive (i.e. at high irradiance and at low irradiance and low C_i) k_N was about 50% lower in Npq4-9$^-$ than in the WT. Consistent with the results of Fig. 4, k_N was significantly higher for the mutant when photosynthesis was limited

Table 1 Comparison of parameters relevant to photosynthesis in *Arabidopsis thaliana* wild type Landsberg *erecta* (WT) and Npq4-9$^-$. Note that R_d (mitochondrial respiration in the light) was calculated from the slope of the dependence of net CO_2 assimilation versus C_i at limiting CO_2 levels. Values of R_n (dark respiration) were based on the steady-state rate of CO_2 evolution following several minutes of darkness. For further details regarding measurement of stomatal resistance (r_s) and other gas-exchange parameters see *Materials and methods* and Laisk and Oja (1998). The PSI fluorescence offset was assessed from measurements of F_{0d} and F_{md} in both the red and far-red spectral ranges of the ED-101BL emitter-detector unit using leaves that had been dark-adapted for 12 h (Genty et al. 1990). *N*, Number of replicate leaves of each line. Effects of genotype on means (±SE) were based on a *t*-test (*, $P < 0.05$; **, $P < 0.01$)

Parameter	WT	Npq4-9$^-$	N
Stomatal Resistance, r_s (s mm^{-1})			
Low light	0.485 ± 0.009	0.486 ± 0.009	3
High light	0.488 ± 0.011	**0.570 ± 0.011	3
Day respiration, R_d (μmol CO_2 m^{-2} s^{-1})	0.044 ± 0.020	0.077 ± 0.042	3
Night respiration, R_n (μmol CO_2 m^{-2} s^{-1})	0.75 ± 0.12	0.75 ± 0.12	6
Leaf absorption coefficient, α	0.801 ± 0.013	0.772 ± 0.006	6
Maximum PSII quantum yield			
(F_v/F_{md})	0.846 ± 0.003	**0.816 ± 0.009	10
$\phi(O_2)$	0.0832 ± 0.0037	*0.0650 ± 0.0047	7
PSI fluorescence (% of F_{0d})	30.1 ± 2.9	28.4 ± 0.9	5
Total Chl (mg m^{-2})	217.9 ± 13.7	187.2 ± 13.2	7
Pigment distribution [mmol (mol Chl *a*)$^{-1}$]			
Neoxanthin	53.9 ± 3.1	48.6 ± 3.9	16
Lutein	147.3 ± 5.0	139.6 ± 2.7	16
Chl *b*	340.4 ± 6.0	335.9 ± 3.9	16
β-Carotene	43.1 ± 2.7	45.5 ± 2.0	16
Viol + Anth + Zea	60.5 ± 2.5	61.6 ± 3.4	16

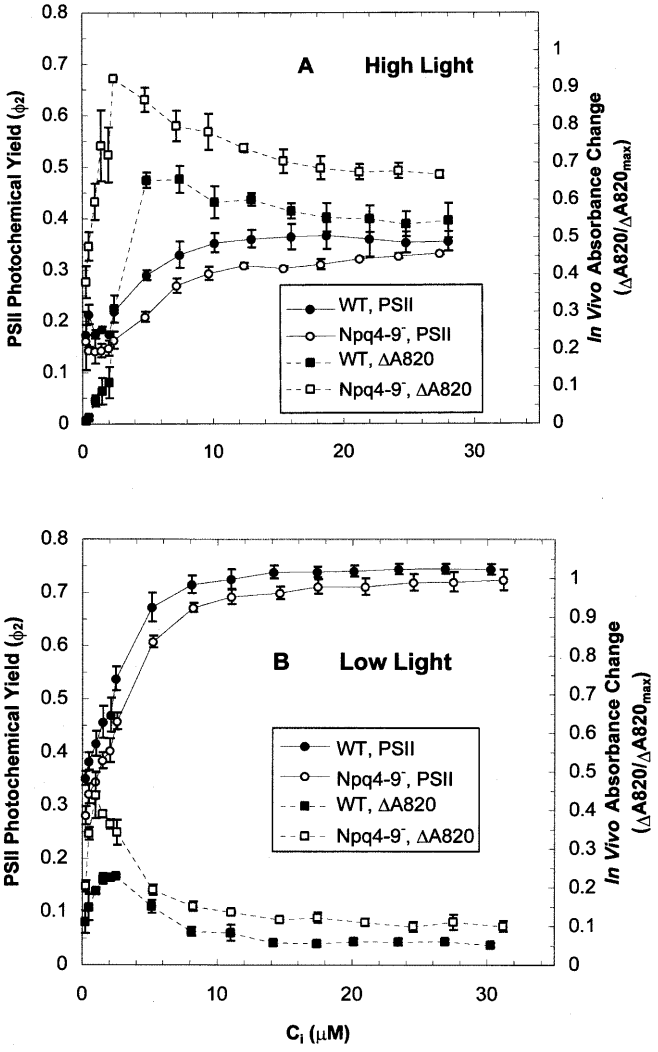

Fig. 3 Dependence of PSII photochemical yield (ϕ_2) on C_i for WT and Npq4-9⁻ *Arabidopsis* at two illumination levels [incident irradiances of 510 (**A**) and 110 μmol quanta $m^{-2}s^{-1}$ (**B**)]. Also shown are parallel measurements of steady-state accumulation of $P700^+$ as indicated by the light-dependent in vivo absorbance at 820 nm ($\Delta A820/\Delta A820_{max}$). Each point is a mean based on measurements from three replicate leaves, and error bars indicate ±SE in this and subsequent figures

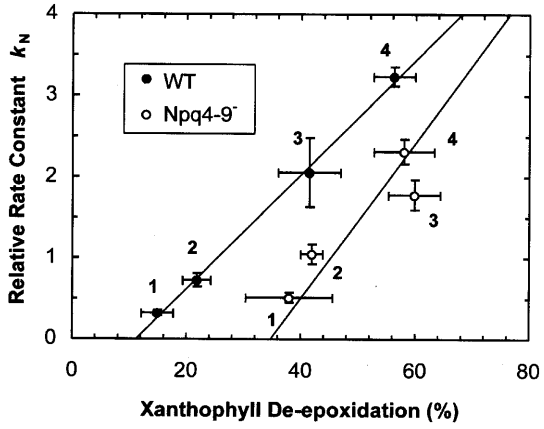

Fig. 4 Relationship between nonphotochemical quenching (k_N, Eq. 4) and xanthophyll de-epoxidation for WT and Npq4-9⁻. Measurements were based on a 10- to 20-min exposure to various irradiance levels. Following fluorescence measurements, samples were quickly frozen in liquid N_2 pending pigment analysis by HPLC. The numerical designation by each point refers to the incident irradiance employed (levels *1–4* correspond to 160, 330, 750, and 1,300 μmol quanta m^{-2} s^{-1}, respectively). The gas phase was air and leaf temperature was 23 °C. Xanthophyll de-epoxidation was calculated as 100 × [Zea + 0.5Anth]/[Viol + Anth + Zea]. Experimental protocols and pigment determination are described in Peterson and Havir (2000). Means shown are the average of four replicates

by availability of quanta (i.e., low irradiance and high C_i values). Corresponding values of k_{P0} (Eq. 3) obtained from these experiments show a slight, yet similar, rise in the magnitude of k_{P0} with increasing C_i at both irradiance levels for the WT. However, CO_2 concentration and irradiance appear to interact with respect to effects on k_{P0} for Npq4-9⁻. The relative increase in k_{P0} with C_i for the mutant at low irradiance was similar to that of WT. However, at high irradiance, maximal k_{P0} values were observed at very low and very high C_i levels for the mutant. This is most likely explained in terms of a latent response to changes in the gas phase CO_2 levels during the course of the measurements. Nevertheless, two-way ANOVA indicated that the average relative decrease in the magnitude of k_{P0} due to the mutation was 12% and 35% across all C_i levels at low and high irradiance, respectively ($P < 0.01$). Substantial down-regulation of PSII quantum yield normally occurs by reduction of electron acceptor pools resulting in closure of centers with respect to further stabilized charge-separation events. Such closure is not reflected in the magnitude of k_{P0} but is manifested as a lowering of the measured fraction of open centers, q_P. Values of q_P (not shown) declined similarly with decreasing C_i for both WT and Npq4-9⁻. However, mean values (±SE) of q_P averaged across all C_i levels at high irradiance were 0.46 ± 0.02 and 0.39 ± 0.02 for WT and mutant, respectively. Corresponding means at low irradiance were 0.82 ± 0.02 and 0.75 ± 0.03. Effects of *npq4-9* on q_P were statistically significant ($P < 0.01$) at each irradiance level and indicate that PSII acceptors were more reduced for the mutant than for the WT.

The dependencies of mean values of k_{P0} on corresponding values of k_N for the experiments of Fig. 5 are shown in Fig. 6. Initial values of k_{P0} (squares) were calculated from F_{0d} and F_{md} values measured for these leaves. As would be expected if the antenna system were the primary locus of reversible thermal conversion, values of k_{P0} for the WT showed only a very slight decline with increasing k_N. In contrast, a strong linear decline in k_{P0} with increasing k_N was observed for Npq4-9⁻. This decline was preceded by development of a small (≈0.4) level of k_N that was not accompanied by a change in k_{P0}. Extrapolation of the linear fit to the data indicated that when PSII is fully quenched in the mutant (i.e. $k_{P0} = 0$) the magnitude of k_N is 2.7. Changes in k_{P0} associated with duration of exposure to

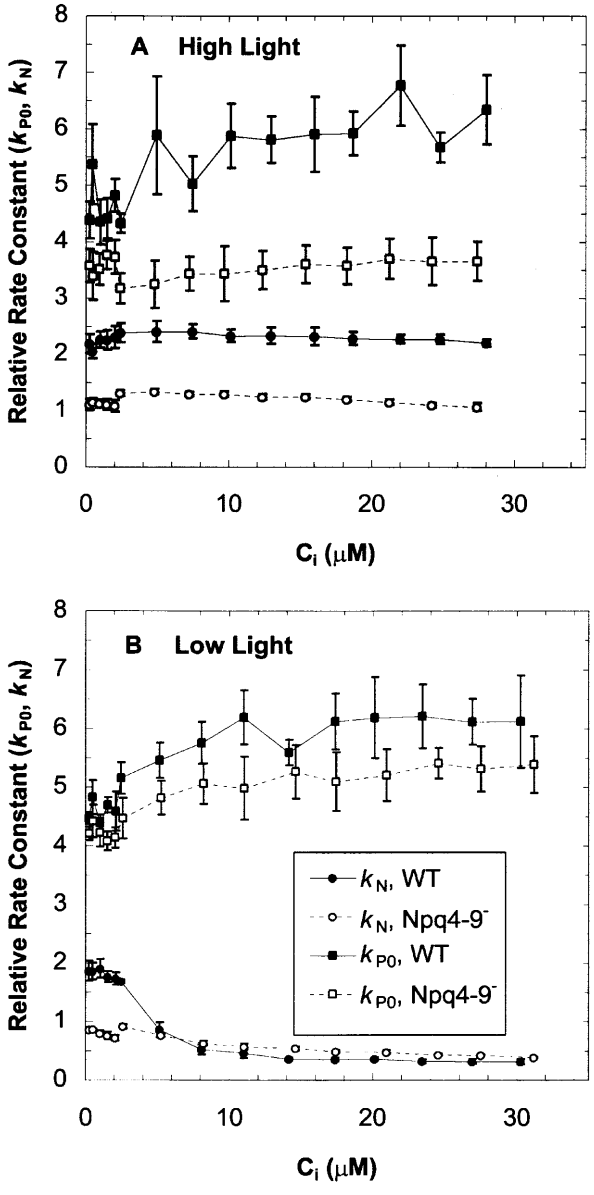

Fig. 5A, B Interactive effects of irradiance level and leaf internal CO_2 concentration (C_i) on the relative rate constants for photochemistry in open PSII centers (k_{P0}, squares) and nonphotochemical quenching (k_N, circles) for WT and Npq4-9⁻. Data were collected in parallel with the measurements of Fig. 3

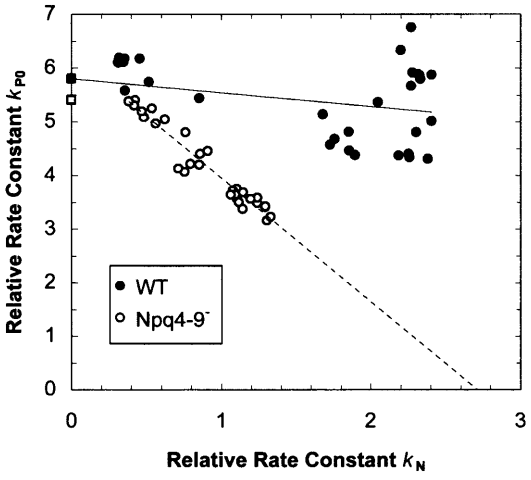

Fig. 6 Comparisons of changes in the magnitude of k_{P0} and k_N for WT and Npq4-9⁻. The lines are linear regression fits to the data (*circles*) obtained from the experiments of Fig. 5. The *squares* on the left axis show k_{P0} values computed from F_{0d} and F_{md} values measured using the same WT and mutant leaves. Note that a slight decline in k_{P0} with increasing k_N was evident for WT. Coefficients of determination were 0.14 ($P < 0.05$) and 0.93 ($P < 0.001$) for WT and mutant, respectively. The k_{P0} values corresponding to the dark-adapted state were not included in the regression analyses

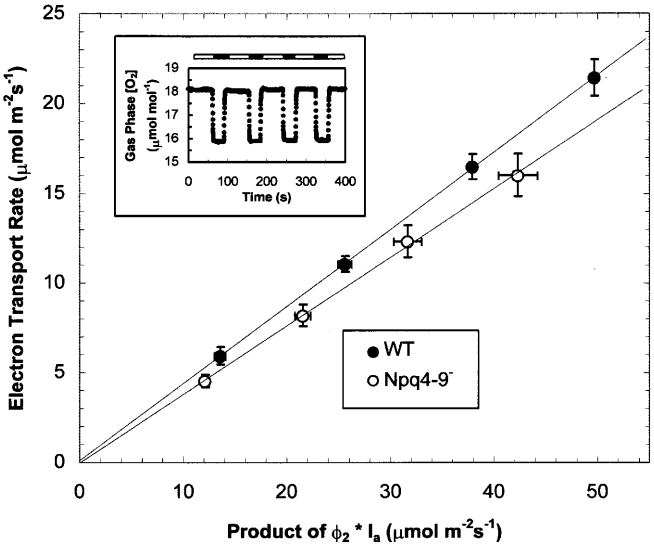

Fig. 7 Relationship between PSII electron transport rate and ($\phi_2 \times I_a$) used to determine the PSII absorption cross-section (a_2) in WT and Npq4-9⁻ (see Eq. 1). The *solid lines* are linear regression fits to the non-averaged data (six replicates per line). Coefficients of determination were 0.94 and 0.89 for WT and Npq4-9⁻, respectively ($P < 0.01$). The slopes (±SE) of the fits were 0.432 ± 0.009 and 0.382 ± 0.011 for WT and Npq4-9⁻, respectively. The *inset* shows a typical recording of the O_2 analyzer response to consecutive light-dark cycles (*white* and *black bars*, respectively) for a WT leaf. Rates of electron transport were calculated as $4f[\Delta O_2]/s$ where f is the gas flow rate (0.5 mmol s^{-1}), s is leaf area (m^2), and $[\Delta O_2]$ is the light-dark change in gas phase O_2 concentration (μmol mol^{-1})

high light were slight and independent of genotype. The extent of decline in k_{P0} (as measured at $C_i = 7.5$ μM) over a period of approximately 1 h in the experiments of Fig. 5A was about 7%.

Figure 7 shows a highly linear dependence of J_t on $\alpha\phi_2 I_o$ (Eq. 1) for WT and Npq4-9⁻ plants in limiting light. Measurements of J_t were based on O_2 evolution at a very low gas phase $[O_2]$, conditions in which photoreduction of O_2 should be negligible. The slopes of plots obtained for individual leaves were employed to assess a_2. A *t*-test revealed that respective mean values of a_2 for the WT and Npq4-9⁻ did not differ significantly ($P > 0.10$). Hence, we accepted the hypothesis that a_2 is unaffected by *npq4-9* and used an overall average of 0.40 (SE = 0.02) to calculate J_t. Rates of total linear electron transport (J_t, Eq. 1) and

electron transport specifically devoted to carbon metabolism (J_c, Eq. 2) with increasing C_i are compared in Fig. 8 for the WT and Npq4-9$^-$. We note that Eq. 2 neglects the aggregate diffusion resistance associated with CO_2 movement through the intercellular air spaces and the liquid phase separating the mesophyll cell wall from the chloroplast stroma. Although the magnitude of this "mesophyll resistance" (r_m) cannot be measured with certainty it is probably significantly less than r_s (Laisk and Loreto 1996). Effects of r_m on J_c were assessed by substituting trial values of C_c [$=(C_i - r_m A)$] for C_i in Eq. 2. At the low gas-phase O_2 levels employed in this study, reasonable values of r_m failed to significantly affect the magnitude of J_c.

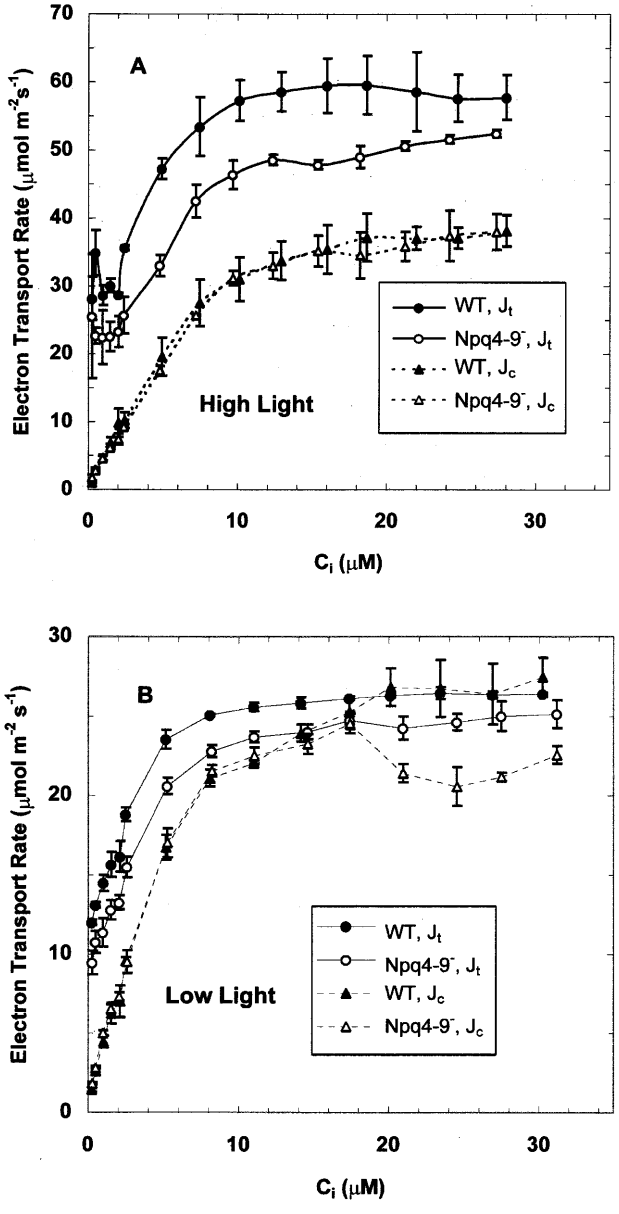

Fig. 8 Relationship between rates of total linear electron transport (J_t, Eq. 1) and electron transport devoted only to photosynthesis plus photorespiration (J_c, Eq. 2) at high (**A**) and low (**B**) irradiance. Note that a value for K_s (23 °C) of 105 was used in Eq. 2 based on measurements of the temperature dependence of the CO_2 compensation point in *Arabidopsis* (data not shown). Results were based on measurements presented in Figs. 3 and 5

The dependence of J_c on C_i was essentially identical for WT and Npq4-9$^-$ at high light and up to 17 μM CO_2 in low light. Conversely, the magnitude of J_t was generally higher for the WT relative to Npq4-9$^-$. Two-way ANOVA indicated that *npq4-9* lowered J_t by an average of 11% and 19% at low and high light, respectively ($P < 0.01$). Clearly, the mutant phenotype was associated with diminished partitioning of electron flow to alternate acceptors [i.e., $(J_t - J_c)/J_t$]. In high light the average proportion of total electron transport associated with reduction of alternate acceptors was 58% in the WT versus 50% in the mutant. Although this difference was significant ($P < 0.01$), effects of C_i on $(J_t - J_c)/J_t$ were much larger.

Discussion

Under conditions of low light and non-limiting CO_2 levels, Npq4-9$^-$ exhibited significantly higher NPQ (i.e. k_N) and a substantially higher degree of xanthophyll de-epoxidation than the WT (Figs. 4 and 5B). Enhancement of NPQ by [Anth + Zea] was sharply lower in the mutant under all conditions tested, however (Fig. 4). Numerous studies point to the important role that the structure of the PSII light-harvesting complex (LHCII) plays in regulating NPQ and xanthophyll cycle activity. Chl *b*-deficient (*chlorina*) mutants of barley exhibit selective loss of specific LHCII proteins but normal levels of PSII-S (Bossmann et al. 1997). Furthermore, levels of xanthophyll cycle intermediates in *chlorina* mutants show a dramatic increase in proportion to total Chl levels (Falbel et al. 1994). Analogous to Npq4-9$^-$, the *chlorina 3613* mutant of barley showed a reduced level of NPQ relative to [Anth + Zea] accumulation (Lokstein et al. 1994; Härtel et al. 1996). Variation in the extent of xanthophyll de-epoxidation in *chlorina* mutants has been interpreted in terms of multiple pools of Viol in normal thylakoids that differ in accessibility to the de-epoxidase (Falbel et al. 1994). In the case of Npq4-9$^-$, an altered PSII-S protein may modify the conformation of the LHCII and thereby eliminate the basis for compartmentation of Viol pools. Alternatively, an altered PSII-S protein may cause a change in the conformation of a complex of the de-epoxidase and the LHCII, thereby affecting the equilibrium constant governing the in vivo concentrations of Viol, Anth, and Zea. Yet another explanation is that since Viol de-epoxidase possesses a pH optimum of 5, higher xanthophyll de-epoxidation in the mutant could be a result of a lower lumenal pH (Siefermann and Yamamoto 1975).

An important result of this study is the demonstration that the relationship between k_{P0} and k_N is profoundly altered by *npq4-9* (Fig. 6). Considerable evidence indicates that NPQ normally occurs due to H^+- and Zea-dependent shifts in LHCII conformation

as opposed to charge recombination processes involving the reaction center (Horton et al. 1996). This implies that changes in energy utilization in the antenna should be unrelated to the intrinsic photochemical capacity of open PSII reaction centers. The very weak dependence of k_{P0} on k_N for the WT indicates that the antenna quenching mechanism is predominant. However, the pronounced linear decline in k_{P0} with increasing k_N in the mutant suggests an involvement of the PSII reaction center in the quenching mechanism. A model involving interconversion of the PSII reaction center between photochemically active and inactive states has been proposed to account for high-energy quenching (Weis and Berry 1987; Krieger and Weis 1993). Low lumen pH was found to cause displacement of Ca^{2+} from PSII resulting in a restriction in electron flow on the donor side (Krieger and Weis 1993). This was accompanied by a 160-mV increase in the midpoint redox potential of Q_A, the primary quinone electron acceptor of PSII. It was suggested that an energy-dissipating recombination of $P_{680}{}^+$ and $Q_A{}^-$ would then be the favored pathway for electron flow in PSII. Reaction-center quenching may occur when antenna quenching is inhibited or becomes saturated. The small initial increase in k_N independent of a change in k_{P0} for the mutant (Fig. 6) could represent quenching associated with direct binding of H^+ by inner antenna Chl-proteins (Gilmore et al. 1998). We note that the magnitude of k_{P0} is highly sensitive to the value of F_0' (or F_{0d}) employed (Eq. 3). Invariant emission from PSI occurs at a level equivalent to 30% of the measured F_{0d} signal in C_3 plants such as *Arabidopsis* (Table 1; Genty et al. 1990; Pfündel 1998). Although correction for PSI fluorescence is seldom applied in other studies, the PSI offset was subtracted from all measured fluorescence yields in these experiments. We emphasize that meaningful estimates of k_{P0} must be based on fluorescence measurements that are free of the PSI signal.

Lumen acidification has been implicated in a PSII inactivation mechanism that was dependent upon integrated photon absorption possibly involving oxidizing radicals (Hurry et al. 1996). Nevertheless, in these experiments we could not detect an interaction between the state of the PSII-S protein and illumination history with regard to PSII reaction-center function as indicated by k_{P0}. The k_N levels of Fig. 4 were attained after comparatively short periods of illumination, consistent with a direct role for the ΔpH in inducing NPQ in both WT and mutant plants. Recent results indicate that enhanced susceptibility to active oxygen species is not necessarily a result of reduced NPQ capacity but instead is associated with a loss in capacity for direct destruction of singlet O_2 as mediated by Anth + Zea. Hence, the Viol de-epoxidase-deficient mutant Npq1-1$^-$ can exhibit effects of enhanced peroxidation in strong light (Havaux et al. 2000). Conversely, the NPQ-deficient PSII-S deletion mutant Npq4-1$^-$, which, like Npq4-9$^-$, retains normal xanthophyll cycle activity, also exhibits a high tolerance to excessive light (Havaux et al. 2000). Hence, the available evidence does not support involvement of singlet O_2 in the transformation of PSII centers from the active to inactive form in Npq4-9$^-$.

Apparent NADPH consumption during combined turnover of the Calvin cycle and photorespiratory pathway (J_c) was identical in WT and Npq4-9$^-$ in high light and at rate-limiting CO_2 levels in low light. Nevertheless, rates of total electron transport (J_t) were consistently lower in the mutant (Fig. 8). Hence, diminished electron-transport capacity in the mutant usually affected only the allocation of reducing equivalents to alternate acceptors. The importance of alternate electron transport pathways to maintenance of high rates of carbon assimilation has been demonstrated recently (Backhausen et al. 2000). Coupled cyclic electron transport around PSI and linear electron transport to alternate acceptors are effective ways of providing extra ATP for regeneration of ribulose bisphosphate by the Calvin cycle while avoiding overreduction of the electron transport system. Hence, CO_2 assimilation is limited by the rate of ATP formation, which accounts for the frequently observed lack of competition for reductant between CO_2 and alternate acceptors (Robinson 1986; Backhausen et al. 2000). In these experiments at low light and high C_i levels (≥20 μM), linear electron transport was exclusively devoted to carbon metabolism in the WT as indicated by a coincidence of J_t and J_c (Fig. 8B). It is possible that coupled linear electron transport was capable of providing an adequate NADPH/ATP for CO_2 assimilation. Any deficit in availability of ATP for CO_2 assimilation caused by alternate biosynthetic processes in the chloroplast or leakage of H^+ across the thylakoid membrane was apparently offset by coupled cyclic electron transport in PSI. In contrast, it appears that these mechanisms were not adequate to maintain high J_c levels at low light and high C_i levels (>20 μM) in the mutant. Indeed, the occurrence of lower J_c values under these conditions was associated with diversion of electron flow to other acceptors, indicative of flexibility in maintaining balanced ATP and NADPH production. Accordingly, a recent model emphasizes the role of redox thresholds involving PSI carriers in the regulation of pathways of electron flow to different acceptors (i.e., plastoquinone, oxaloacetate, NO_2^-, O_2, CO_2) that could differ in H^+:e^- stoichiometry (Backhausen et al. 2000). The redox state of the PSI acceptor side is a result of electrochemical equilibria with carriers such as pyridine nucleotides and P700. It is significant, therefore, that differing patterns of allocation of electrons to various acceptors for the WT and Npq4-9$^-$ are associated with contrasts in regulation of the redox state of the PSI donor P700.

Measurements of ΔA820 have been frequently employed to probe light utilization in PSI and the cooperation of both photosystems during linear electron transport from H_2O to NADP (Weis and Lechtenberg 1989; Foyer et al. 1990; Peterson 1991). Dissipation of excess quanta as heat by $P700^+$ contrasts with the

photoprotective antenna-based processes that occur in PSII. The steady-state concentration of $P700^+$ is a result of the regulated rate of electron donation from plastoquinol to $P700^+$ (photosynthetic control) versus the rate of photooxidation of P700. The higher $P700^+$ levels consistently observed for the mutant could be due to a larger absorption cross-section for PSI. However, the PSII absorption cross-section (a_2, see above) and Chl a/b level (Table 1) were unaffected by the mutation so it is unlikely that the PSI absorption cross-section was altered. Maximum steady-state accumulation of $P700^+$ occurred at CO_2 levels ≤ 5 μM (Fig. 3). As the C_i increased there was a progressive shift to a lower degree of oxidation (Fig. 3) associated with an increase in allocation of electrons to ATP-consuming carbon metabolism (Fig. 8). The ensuing decline in ΔpH would decrease the resistance to plastoquinol oxidation by Cyt b_6f allowing an increased flow of electrons to $P700^+$ (Harbinson and Hedley 1989; Foyer et al. 1990). The decline in levels of $P700^+$ at very low C_i levels is due to blockage of P700 photooxidation by reduced acceptors (Laisk and Oja 1995). Nevertheless, the relative increase in oxidation of the PSI donor in the mutant compared to the WT is highest under these conditions, consistent with differential effects on inter-photosystem electron transport. The PSII acceptor side was under all conditions more reduced (lower q_P) and the PSI donor side was more oxidized (higher $\Delta A820/\Delta A820_{max}$) in the mutant. This indicates a greater resistance to electron flow from plastoquinol to $P700^+$. Higher $P700^+$ levels in the mutant may result from maintenance of a higher ΔpH, altered sensitivity to the ΔpH, or a change in the interaction between the plastoquinone pool and the PSII acceptor side involving a shift in the midpoint redox potential of Q_A (Krieger and Weis 1993). It is unclear at this time how the *npq4-9* mutation alters both the NPQ mechanism and control of electron flow between PSII and PSI.

Acknowledgements We thank Krishna Niyogi and Alba Phippard for performing the DNA sequencing and providing the antibody against PSII-S. We also extend thanks to Neil Schultes for helpful discussions and to Carol Clark for skillful technical assistance.

References

Backhausen JE, Kitzmann C, Horton P, Scheibe R (2000) Electron acceptors in isolated intact chloroplasts act hierarchically to prevent over-reduction and competition for electrons. Photosynth Res 64:1–13

Bossmann B, Knoetzel J, Jansson S (1997) Screening of chlorina mutants of barley (*Hordeum vulgare* L.) with antibodies against light-harvesting proteins of PSI and PSII. Absence of specific antenna proteins. Photosynth Res 52:127–136

Dau H (1994) Molecular mechanisms and quantitative models of variable photosystem II fluorescence. Photochem Photobiol 60:1–23

Demmig B, Winter K, Krüger A, Czygan F-C (1987) Photoinhibition and zeaxanthin formation in intact leaves: a possible role of the xanthophyll cycle in the dissipation of excess light. Plant Physiol 84:218–224

Falbel TG, Staehelin LA, Adams WW III (1994) Analysis of xanthophyll cycle carotenoids and chlorophyll fluorescence in light intensity-dependent chlorophyll-deficient mutants of wheat and barley. Photosynth Res 42:191–202

Foyer C, Furbank R, Harbinson J, Horton P (1990) The mechanisms contributing to photosynthetic control of electron transport by carbon assimilation in leaves. Photosynth Res 25:83–100

Funk C, Schröder WP, Napiwotzki A, Tjus SE, Renger G, Andersson B (1995) The PSII-S protein of higher plants: a new type of pigment-binding protein. Biochemistry 34:11133–11141

Genty B, Briantais J-M, Baker NR (1989) The relationship between the quantum yield of photosynthetic electron transport and quenching of chlorophyll fluorescence. Biochim Biophys Acta 990:87–92

Genty B, Wonders J, Baker NR (1990) Non-photochemical quenching of F_0 in leaves is emission wavelength dependent: consequences for quenching analysis and its interpretation. Photosynth Res 26:133–139

Gilmore AM, Shinkarev VP, Hazlett TL, Govindjee (1998) Quantitative analysis of the effects of intrathylakoid pH and xanthophyll cycle pigments on chlorophyll *a* fluorescence lifetime distributions and intensity in thylakoids. Biochemistry 39:13582–13593

Harbinson J, Hedley CL (1989) The kinetics of P-700^+ reduction in leaves: a novel in situ probe of thylakoid functioning. Plant Cell Environ 12:357–369

Härtel H, Lokstein H, Grimm B, Rank B (1996) Kinetic studies on the xanthophyll cycle in barley leaves. Influence of antenna size and relations to nonphotochemical quenching. Plant Physiol 110:471–482

Havaux M, Bonfils J-P, Lütz C, Niyogi KK (2000) Photodamage of the photosynthetic apparatus and its dependence on the leaf developmental stage in the *npq1* arabidopsis mutant deficient in the xanthophyll cycle enzyme violaxanthin de-epoxidase. Plant Physiol 124:273–284

Horton P, Ruban AV, Walters RG (1996) Regulation of light harvesting in green plants. Annu Rev Plant Physiol Plant Mol Biol 47:655–684

Hurry V, Anderson JM, Badger MR, Price GD (1996) Reduced levels of cytochrome b_6/f in transgenic tobacco increases the excitation pressure on photosystem II without increasing sensitivity to photoinhibition in vivo. Photosynth Res 50:159–169

Jansson S (1999) A guide to the *Lhc* genes and their relatives in *Arabidopsis*. Trends Plant Sci 4:236–240

Krieger A, Weis E (1993) The role of calcium in the pH-dependent control of photosystem II. Photosynth Res 37:117–130

Laisk A, Loreto F (1996) Determining photosynthetic parameters from leaf CO_2 exchange and chlorophyll fluorescence: Rubisco specificity factor, dark respiration in the light, excitation distribution between photosystems, alternative electron transport and mesophyll diffusion resistance. Plant Physiol 110:903–912

Laisk A, Oja V (1995) Coregulation of electron transport through PSI by Cyt b_6f, excitation capture by P700 and acceptor side reduction. Time kinetics and electron transport requirement. Photosynth Res 45:11–19

Laisk A, Oja V (1998) Dynamics of leaf photosynthesis. Rapid response measurements and their interpretations. CSIRO, Australia

Laisk A, Oja V, Rasulov B, Eichelmann H, Sumberg A (1997) Quantum yields and rate constants of photochemical and nonphotochemical excitation quenching. Experiment and model. Plant Physiol 115:803–815

Li X-P, Björkman O, Shih C, Grossman AR, Rosenquist M, Jansson S, Niyogi KK (2000) A pigment-binding protein essential for regulation of photosynthetic light harvesting. Nature 403:391–395

Lokstein H, Härtel H, Hoffmann P, Woitke P, Renger G (1994) The role of light-harvesting complex II in excess excitation energy dissipation: an in-vivo fluorescence study on the origin of high-energy quenching. Photochem Photobiol B 26:175–184

Melis A (1999) Photosystem-II damage and repair cycle in chloroplasts: What modulates the rate of photodamage in vivo?. Trends Plant Sci 4:130–135

Niyogi KK, Björkman O, Grossman AR (1997) *Chlamydomonas* xanthophyll cycle mutants identified by video imaging of chlorophyll fluorescence quenching. Plant Cell 9:1369–1380

Niyogi KK, Grossman AR, Björkman O (1998) *Arabidopsis* mutants define a central role for the xanthophyll cycle in the regulation of photosynthetic energy conversion. Plant Cell 10:1121–1134

Peterson RB (1991) Effect of O_2 and CO_2 concentrations on quantum yields of photosystems I and II in tobacco leaf tissue. Plant Physiol 97:1388–1394

Peterson RB, Havir EA (2000) A nonphotochemical quenching-deficient mutant of *Arabidopsis thaliana* possessing normal pigment composition and xanthophyll cycle activity. Planta 210:205–214

Pfündel E (1998) Estimating the contribution of photosystem I to total leaf chlorophyll fluorescence. Photosynth Res 56:185–195

Pogson BJ, Niyogi KK, Björkman O, DellaPenna D (1998) Altered xanthophyll compositions adversely affect chlorophyll accumulation and nonphotochemical quenching in *Arabidopsis*. Proc Natl Acad Sci USA 95:13324–13329

Robinson JM (1986) Carbon dioxide and nitrite photoassimilation processes do not intercompete for reducing equivalents in spinach and soybean leaf chloroplasts. Plant Physiol 80:676–684

Schreiber U, Klughammer C, Neubauer C (1988) Measuring P700 absorbance changes around 830 nm with a new type of modulation system. Z Naturforsch Teil C 43:686–698

Siefermann D, Yamamoto HY (1975) Properties of NADPH and oxygen-dependent zeaxanthin epoxidation in isolated chloroplasts. A transmembrane model for the violaxanthin cycle. Arch Biochem Biophys 171:70–77

Weis E, Berry JA (1987) Quantum efficiency of photosystem II in relation to "energy" dependent quenching of chlorophyll fluorescence. Biochim Biophys Acta 894:198–208

Weis E, Lechtenberg D (1989) Fluorescence analysis during steady-state photosynthesis. Philos Trans R Soc Lond Ser B 323:252–268